

1 **Sorption of inorganic radiocarbon on iron oxides**

2 Janne Lempinen, Eveliina Muuri, Merja Lusa, Jukka Lehto

3 *Department of Chemistry – Radiochemistry,*

4 *P.O.Box 55, FIN-00014 University of Helsinki, Finland*

5 **Abstract**

6 The sorption of inorganic radiocarbon on goethite, hematite and magnetite was studied as
7 a function of carbon concentration, pH and ionic strength. It was discovered that the
8 sorption of radiocarbon on magnetite was negligible in all studied conditions. The
9 distribution coefficients of radiocarbon on hematite and goethite decreased with
10 increasing pH whereas the ionic strength had only a slight decreasing effect on
11 radiocarbon sorption. The sorption on goethite and hematite was modelled with PhreeqC
12 using a generalized double-layer surface complexation model.

13 **Keywords**

14 radiocarbon, sorption, nuclear waste, goethite, hematite, magnetite

15 **Introduction**

16 Radiocarbon, ^{14}C , is assumed to be the most critical radionuclide, in addition to ^{36}Cl and
17 ^{129}I , with respect to prospective radiation doses to human resulting from the final disposal
18 of spent nuclear fuel in the future [1]. ^{14}C is a pure beta emitter and the maximum energy
19 of its beta particles is 156 keV with a half-life of 5730 years. In Finland, the spent nuclear
20 fuel will be disposed of at the depth of about 400 meters in a bedrock repository. The
21 disposal will not include fuel reprocessing and thus the material to be disposed of consists
22 of the actual fuel material, i.e. irradiated uranium dioxide, as well as the Zircaloy
23 cladding and the metallic parts of the fuel assembly. In these, ^{14}C is produced when

24 neutrons activate the nitrogen in the materials with the reaction $^{14}\text{N}(n,p)^{14}\text{C}$. It can be
25 found in the fuel material, Zircaloy cladding and steel structures in approximately equal
26 portions [2]. Furthermore, one tenth of radiocarbon is assumed to occur in the easily
27 soluble instant release fraction in fuel rod gaps and grain boundaries of the spent nuclear
28 fuel [3]. The chemical forms of ^{14}C in the fuel and metallic structures are still unclear but
29 it is assumed to occur as sparingly soluble carbide and elemental carbon [4-6]. Radiolysis
30 caused by the radiation from the nuclear fuel may, however, oxidize these sparingly
31 soluble species into more soluble species, for instance, carbon dioxide.

32 Very reducing conditions are prevailing at the Olkiluoto final disposal depth of
33 approximately 400 meters, which implies that the plausible oxidation state of carbon is –
34 IV and that the chemical form of carbon is methane and partly higher hydrocarbons. The
35 study of Pitkänen and Partamies [7] has confirmed this when they determined the
36 chemical forms of dissolved carbon in the groundwater of Olkiluoto. While dissolved
37 carbon in the surface soil and in the upper parts of the bedrock is mainly as carbonate, its
38 concentration being up to 80 mg/l, the methane concentrations in these layers are very
39 low at concentrations less than 1 mL/L. At the disposal depth the situation is vice versa as
40 the carbonate concentration is at a few mg/L and that of methane a few hundred mL/L. It
41 is thus reasonable to assume that if any carbon is released from the fuel as carbon dioxide
42 it will be reduced to methane. Methane dissolved into water will not be retained on the
43 mineral surfaces but it can be transported in water conducting fractures closer to the
44 biosphere and, furthermore, be oxidized to carbonate at layers closer to ground surface. In
45 reality, very little is known about the behavior of ^{14}C in the bedrock and soil. As a result,
46 in the safety analysis it is conservatively presumed that ^{14}C is not retained at all in the
47 bedrock but is transported at the velocity of the groundwater flow.

48 Carbon occurs in the solid state in the bedrock either as calcite (CaCO_3) or graphite,
49 which both are common fracture minerals in the Olkiluoto bedrock together with pyrite
50 and clay minerals, such as kaolinite and illite [8]. In addition, carbon may occur in the
51 bedrock as siderite (FeCO_3). ^{14}C can be retained as carbonate on calcite and siderite
52 through isotope exchange [9-10]. There is constant dissolution and precipitation at equal
53 rates of calcite in solubility equilibrium with groundwater and, thus, also ^{14}C as carbonate

54 ($^{14}\text{CO}_3^{2-}$) in equilibrium with calcite water system will precipitate as carbonate in the
55 system.

56 In addition to calcite and siderite, ^{14}C as carbonate can be retained on the surfaces of iron
57 oxide minerals, the surfaces of which are at least partly positive due to the protonation of
58 the hydroxyl groups [11]. The formation of a monodentate inner-sphere carbonate surface
59 complex has been suggested as a possible adsorption reaction of carbonate on goethite
60 based on ATR-FTIR studies [12-13] whereas bidentate complexation on hematite has
61 been claimed by Brechbühl et al. [14]. Protonation and the positive charge of the minerals
62 surfaces is highly pH dependent: the lower the pH, the higher the positive charge. The
63 surface charge of iron oxides in groundwater in the typical pH range of 8-9 is mostly
64 neutral and thus sorption is presumably low.

65 The sorption of ^{14}C as carbonate in goethite, hematite and magnetite was studied here as a
66 function of carbon concentration. In addition, the effect of competing ions and pH was
67 investigated and the results were modelled with PhreeqC. The isoelectric points (IEP) and
68 the specific surface areas of the studied minerals was determined to support the
69 modelling of the results. The three iron oxides used in this study represent iron oxides at
70 various environmental redox conditions. Magnetite, Fe_3O_4 , is most prevailing in non-
71 oxic conditions and composes of both di- and trivalent iron. The two other oxides,
72 goethite $\alpha\text{-FeOOH}$ and especially hematite $\alpha\text{-Fe}_2\text{O}_3$, containing only trivalent iron, are
73 prevailing in more oxidizing conditions. These two latter are the most abundant iron
74 oxides in soils.

75 **Experimental**

76 **Minerals**

77
78 The mineral powders used in the batch sorption experiments were Alfa Aesar (Ward Hill,
79 MA, USA) produced goethite (α -phase, Powder), hematite (α -phase, nanopowder, 98 %
80 metals basis, 30-50 nm APS Powder) and magnetite (98 % metals basis, 20-30 nm APS

81 Powder). Specific surface areas were measured at the Chalmers University of
82 Technology, Sweden, with the Kr-BET method.

83

84 Batch sorption experiments

85

86 Batch sorption experiments were performed to determine the sorption isotherms for
87 carbonate and to study the effect of pH and ionic strength on the sorption. For sorption
88 isotherms, samples with various concentrations of NaHCO₃ and 0.01 M TRIS buffer
89 (tris(hydroxymethyl)aminomethane) (pH 8.2) were prepared and radiolabeled with 18.5
90 kBq of NaH¹⁴CO₃. The minerals were added into these solutions as suspensions in MilliQ
91 water to achieve a sample volume of 20 mL (Milli-Q[®] system with Quantum[®] polishing
92 cartridge, Merck, Germany). The solid to liquid ratio was 5 g/L and initial ¹⁴C activity
93 concentration 925 Bq/mL. The samples were left to equilibrate under shaking for one
94 week in capped vials. Activity standard for the radioactivity measurement was prepared
95 by adding MilliQ water instead of the mineral-water suspension and background sample
96 by adding stable NaHCO₃ without the tracer.

97

98 After the equilibration period, aliquots of the samples were ultracentrifuged and 0.5 mL
99 subsamples of the supernatants were mixed with 1 mL of 0.1 M NaOH to prevent
100 degassing of HCO₃⁻ as CO₂. Finally, 10 mL of OptiFluor LSC cocktail was added to each
101 sample and the samples were measured for ¹⁴C with Hidex 300 SL liquid scintillation
102 spectrometer. The TDCR (triple-to-double coincidence ratio) was used as a counting
103 efficiency determination method of each sample.

104

105 The fraction of sorbed carbonate ions was calculated from the decrease in the activity
106 concentration of the solution assuming isotopic equilibrium between stable and
107 radioactive carbonate ions.

108 The Langmuir isotherm equation

109

$$q = \frac{q_0 K_L c}{1 + K_L c} \quad (1)$$

110 where q is the sorbed amount (in mol/kg mineral) and c the carbonate ion concentration
111 in the solution was used to find the constants q_0 and K_L that represent the maximum
112 sorption (mol/kg) and equilibrium constant for the sorption reaction, respectively. A non-
113 linear curve fit to the experimental q over c data using fitting equation (1) was performed
114 using OriginPro 8.6 software. Moreover, the surface site density was calculated from the
115 maximum sorption and specific surface area of the minerals.

116 In order to study the effect of pH and ionic strength on the sorption, sets of samples were
117 prepared as described above at three different ionic strengths (0, 0.01 and 0.1 M) using
118 NaCl as the background electrolyte and HCl and NaOH for pH adjustment. The NaHCO_3
119 concentration in the samples was kept at $5 \cdot 10^{-5}$ M and the initial ^{14}C activity
120 concentration at 925 Bq/mL. Also these samples were allowed to equilibrate for one
121 week, which after the samples were ultracentrifuged and supernatant activity was
122 measured as described above.

123 From the activity measurement results, the distribution coefficient K_d was calculated
124 using equation

$$125 \quad K_d = \frac{A_0 - A}{A} \times \frac{V}{m} \quad (2)$$

126 where A_0 and A are the initial and final activity concentrations (Bq) of the solution,
127 respectively, and V and m the sample volume (L) and mass (kg), respectively.

128 The pH values of the remaining suspensions were measured using a glass electrode. For
129 all the sorption isotherm samples, the pH remained constant at 8.2 ± 0.2 . For the pH
130 dependent samples, the samples having a pH value lower than 6.5 were excluded from
131 the results as inorganic radiocarbon may gas out as CO_2 at low pH.

132 As only very low sorption of carbonate on magnetite was observed in studied conditions
133 it is not discussed in detail in the further treatment.

134

135 Zeta potential measurements

136

137 The zeta potentials of goethite and hematite were measured using a Malvern Zetasizer
138 instrument. For these measurements 0.5 g/L suspensions of each mineral was prepared in
139 MilliQ water, 0.01 M NaCl or 0.1 M NaCl. pH of the suspensions was adjusted using

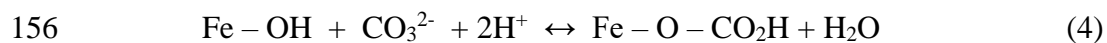
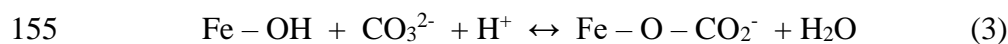
140 0.01 M HCl or NaOH. The solutions were left to equilibrate in capped polyethylene vials
141 for one week before the measurement of zeta potential. Due to what is considered random
142 noise in the zeta potential data, smoothed curves as 5-point moving average were
143 produced using OriginPro 8.6 software in order to find the isoelectric points (IEP) of the
144 minerals.

145

146 Geochemical modelling

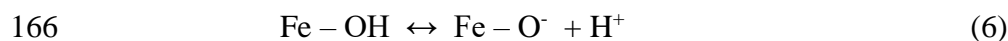
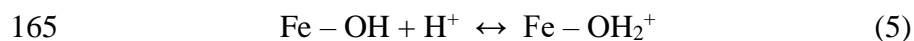
147

148 The sorption of carbonate on goethite and hematite was modelled with PhreeqC
149 Interactive using a generalized double-layer surface complexation model (Dzombak &
150 Morel, 1990) and the phreeqc.dat database. IEP values were obtained from Zeta potential
151 measurements and sorption site densities from Langmuir fitting of the carbonate sorption
152 isotherms. Based on the works of Appello et al. [16], Brechtbühl et al. [14], Villalobos et
153 al. [13] and van Geen et al. [11] on carbonate sorption on hematite and goethite the
154 sorption was considered to consist of two reactions:



157 resulting from ligand exchange reactions of carbonate and bicarbonate ions.

158 In the model, the oxide/water interface is presumed to be composed of two layers of
159 charge: a surface layer and a diffuse layer of counterions in solutions. As a result, all
160 specifically adsorbed ions are assigned to the surface layer, while all non-specifically
161 sorbed counterions are assigned to the diffuse layer [11,17]. The charge of an oxide
162 surface is determined by proton transfer reactions and surface coordination reactions. The
163 dependence of surface charge on pH is attributed to protonation and deprotonation
164 reactions of the surface sites:



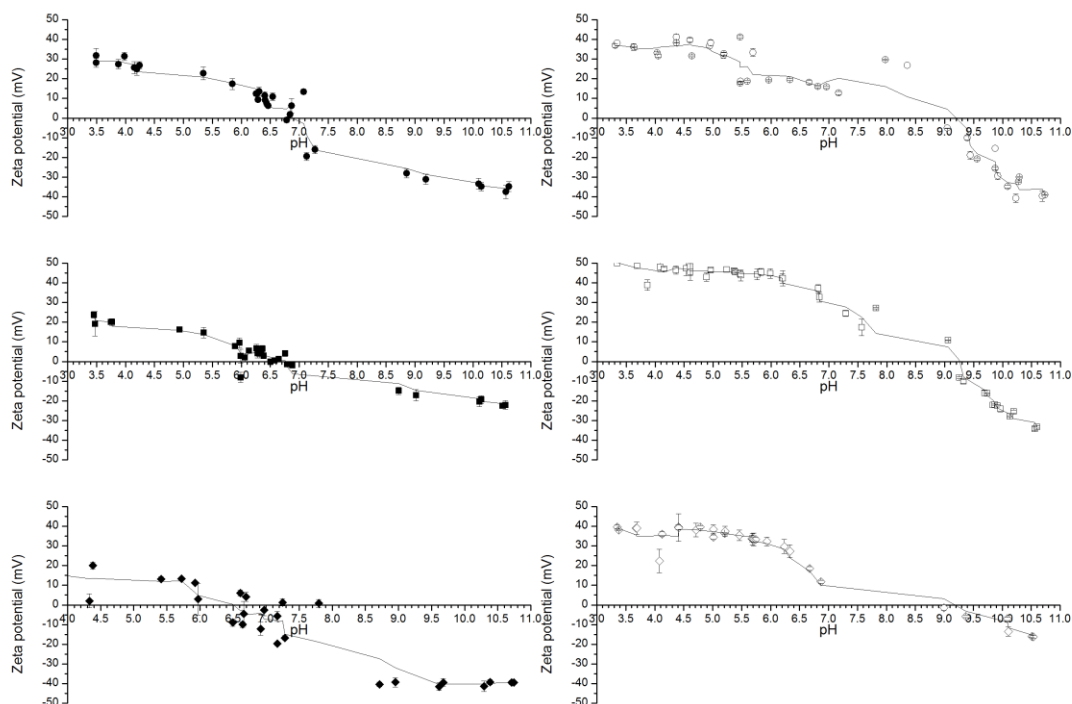
167 Apparent equilibrium constants for these surface species for different minerals can be
168 calculated from zeta potential data as the reactions (5) and (6) are affected by the variable
169 charge of the oxide surface.

170 Using IEP values and sorption site densities, the surface complexation constants of the
171 reactions (3) and (4) were modelled to best fit with the carbonate isotherm data.
172 The CO₂ saturation indices for the solutions in sorption isotherm samples were checked
173 with PhreeqC modelling to fall under -3.42 (corresponding to atmospheric CO₂
174 concentration of 380 ppm). Sorption isotherm data exceeding this SI value was excluded
175 from further calculations because degassing of carbon dioxide from these solutions could
176 not be ruled out.

177 **Results and discussion**

178 Isoelectric points and specific surface areas of the minerals

179
180 The zeta potential of hematite and goethite at three ionic strengths as a function of pH are
181 shown in Fig. 1. The data suffers from irregularities that are considered as noise and the
182 curves show the smoothed data that was used to find the isoelectric point of the minerals.
183 For goethite, the ionic strength had no significant effect on the isoelectric point which
184 was found to fall between pH values 9.1 and 9.3. Here the IEP of goethite is taken as 9.2 ± 0.1 .
185 For hematite, the IEP varied between 6.5 and 6.9, and thus the value 6.7 ± 0.2 was
186 selected for the IEP of hematite. The IEP values determined were used in the modelling
187 of the sorption results. The reported IEP values of iron oxides vary considerably from one
188 product to another, in the range 7.4-9.4 for goethite and 7.0-9.3 for hematite [15]. Our
189 value for hematite lies in the upper end of the range while that of goethite falls below the
190 reported range. Based on the observed values one would assume that hematite would be
191 the most efficient in anion sorption due to its positive surface up to pH 9.3 while goethite
192 would hardly take any anions at relevant groundwater pH values between 7 and 9. This
193 will be discussed later. The reported IEP value for magnetite lies in the range 6.0-6.8
194 being logical with our observation of no carbonate sorption taking place [15]. The
195 measured specific surface area values were $15.8 \pm 0.1 \text{ g/m}^2$, $113 \pm 0.2 \text{ g/m}^2$ and $41.0 \pm$
196 0.1 g/m^2 for goethite, hematite and magnetite, respectively.



198
 199 **Fig. 1** The zeta potentials of hematite (right-hand side) and goethite (left-hand side) as a
 200 function of pH. Hematite in MilliQ water (\circ), 0.01 M NaCl ($!$) and 0.1 M NaCl (Δ) and
 201 goethite in MilliQ water ($-$), 0.01 M NaCl (∇) and 0.1 M NaCl (M). The smoothed
 202 curves show the 5-point moving average of the data.

203

204 Sorption isotherms

205

206 The carbonate sorption isotherms for goethite and hematite were rather similar (Fig. 2).

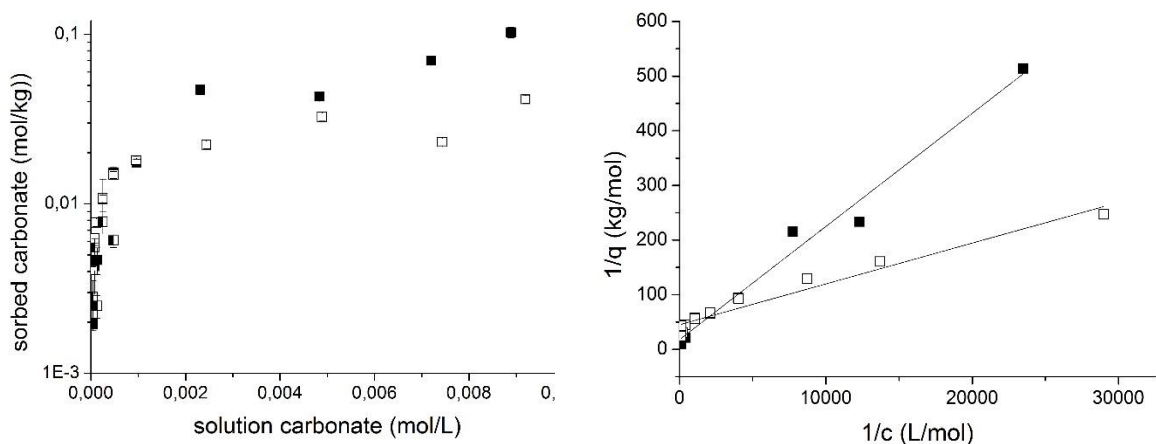
207 The sorption of carbonate on magnetite was at a very low level of about 1 mmol/kg at

208 maximum and thus magnetite is not further discussed. The measured carbonate sorption

209 data of goethite and hematite could be reproduced well with the Langmuir equation as is

210 seen in Figure 2 on the right. The constants q_0 and K_L are given in Table 2 along with the

211 specific surface areas and calculated sorption site densities. For goethite, the pH 8.2 in
 212 the sorption isotherm samples was less than the IEP 9.2 and the surface of the mineral
 213 was thus cationic which favors the sorption of carbonate ions by anion exchange or
 214 surface complexation. However, for hematite the IEP of 6.7 was lower than that in the
 215 batch experiments, which implies an anionic surface for hematite and thus anion
 216 exchange is not a feasible sorption mechanism.



217 **Fig. 2** Sorption isotherms of carbonate ions on hematite (!) and goethite (∇) at pH 8.2 ±
 218 0.2 (left) and Right the Langmuir fittings of the results (right).

219
 220 **Table 2.** The maximum sorption q_0 , sorption equilibrium constant K_L , the adjusted R^2 of
 221 the non-linear curve fit, the specific surface area s and sorption site density d for the
 222 sorption of carbonate ions on hematite and goethite.

Mineral	q_0 (mol/kg)	K_L (L/mol)	Adj. R^2	s (m ² /g)	d (1/nm ²)
Hematite	0.056	660	0.985	113 ± 0.5	0.30
Goethite	0.022	6010	0.959	15.8 ± 0.1	0.84

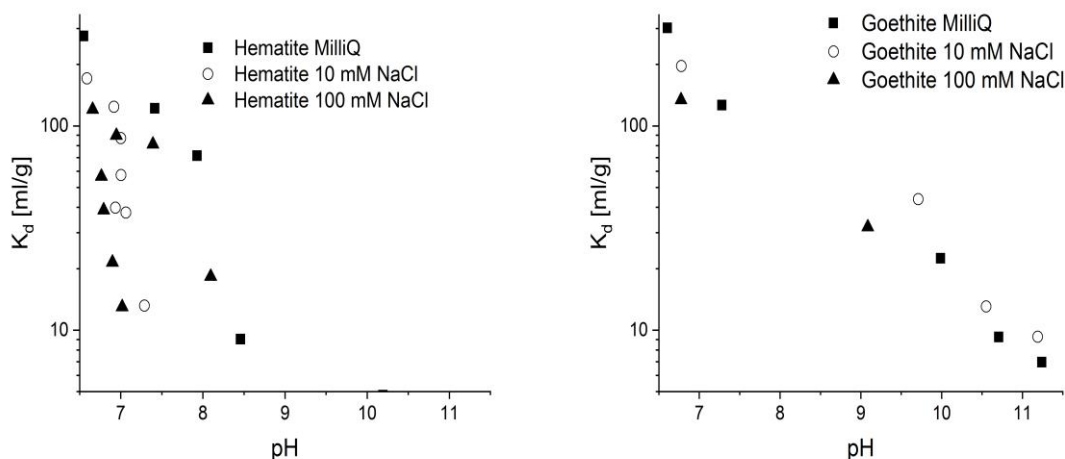
223

224 Effect of ionic strength and pH

225

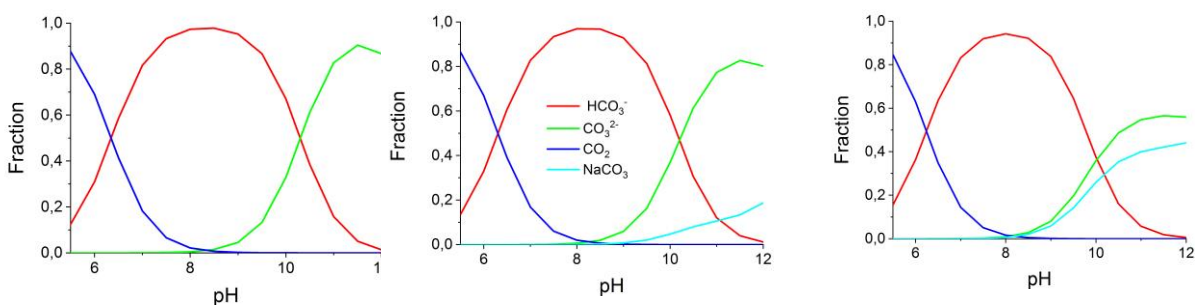
226 At pH 6.5-7.0 the distribution coefficient of carbonate on hematite and goethite were at
227 the same level, at 100-300 mL/g (Fig. 3). At higher pH values K_d decreased
228 systematically, for hematite more drastically, being below 10 mL/g already at pH 8 while
229 for goethite the K_d remained above this value up to pH 10.5. This behavior is logical
230 considering the IEPs of the minerals, 6.7 for hematite and 9.2 for goethite. The declining
231 trend was as expected because the positive charge of the mineral surfaces decreases as the
232 pH increases and thus the sorption of carbonate decreases. Furthermore, as the pH
233 decreases the speciation of carbon changes from carbonate (CO_3^{2-}) to bicarbonate (HCO_3^-)
234) and finally to carbon dioxide (CO_2) (Fig. 4). This decreases the negative charge of the
235 sorbing species and, consequently, decreases the sorption on negatively charged mineral
236 surfaces. Thus, as the pH decreases there are two factors acting to opposite directions:
237 increasing protonation favors sorption while protonation of the carbonate ions diminishes
238 it.

239 The ionic strength had only a slight decreasing effect on the distribution coefficient,
240 which is in line with the fact that sorption mechanism is inner-sphere complexation. The
241 decreasing effect caused by the ionic strength can be due to the saturation of sorption
242 sites caused by the interactions of chloride ions on the plane typically occupied by
243 electrolyte outer-sphere complexes. The negative charge of carbonate complex extending
244 onto the diffuse layer is highly influenced by the electrostatic field created by the
245 adsorption of electrolyte anions, such as chloride ions, on this plane [13]. Therefore, an
246 increase in ionic strength causes an increase of negative charge on this plane and thus a
247 decrease in carbonate adsorption. Furthermore, in higher NaCl concentrations sodium
248 complexes play a more significant role in the speciation of carbon and, at higher pH
249 values NaCO_3^- is a dominating species together with CO_3^{2-} (Fig. 4).



250 **Fig. 3** Distribution coefficients of carbonate on hematite (left) and goethite (right) as a
 251 function of pH in MilliQ, 10 mM NaCl and 100 mM NaCl solutions.

252



253 **Fig. 4** Aqueous speciation of carbon. Left: MilliQ, Middle: 0.01 mM NaCl, Right: 0.1
 254 mM NaCl modelled with PhreeqC. Thermodynamic data from phreeqc.dat was used.
 255

256

257 **Geochemical modelling**

258

259 The sorption results were modelled with PhreeqC using a generalized double-layer
 260 surface complexation model using IEP values obtained from Zeta potential measurements
 261 and the sorption sites densities obtained from specific surface area measurements and the
 262 Langmuir isotherms. Surface complexation constants for the two reactions described in
 263 Equations 3 and 4 were obtained from the best fit with experimental isotherm data (Table
 264 1). As a starting point in modelling of surface complexation constants the values reported

265 by Appelo et al. [16] and Brechbühl et al. [14] were used. The model was able to
 266 reproduce well the pH dependent sorption results of carbonate on goethite, but
 267 underestimated the concentration dependent results (Fig 5). The sorption site density 0.84
 268 sites/nm² used in the model was considerably smaller than 2.31 sites/nm² used by Van
 269 Geen et al. [11] and by Dzombak and Morel [17], which may explain the low modelled
 270 sorption compared to experimentally observed one. However, the fitting of the pH
 271 dependent results would suffer from increasing the sorption site density. The surface
 272 complexation constants obtained from the fitting (12.36 and 20.12) were close to the
 273 values (12.78 and 20.37) obtained by Appelo et al. [16] in a similar study.

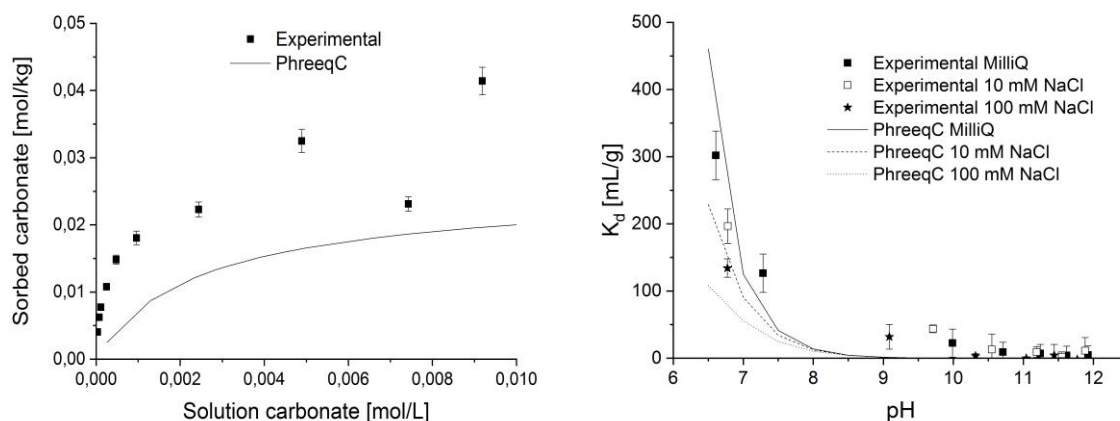
274

275 **Table 1.** *Surface complexation constants for carbonate sorption on goethite and hematite*
 276 *used in this study.*

Surface complexation constants	log K
<i>Surface acid-base reactions on goethite</i>	
Hfo_wOH = Hfo_wOH	0
Hfo_wOH + H ⁺ = Hfo_wOH ₂ ⁺	6.7
<i>Surface acid-base reactions on hematite</i>	
Hfo_wOH = Hfo_wOH	0
Hfo_wOH + H ⁺ = Hfo_wOH ₂ ⁺	9.2
<i>Carbonate sorption on goethite</i>	
Hfo_wOH + CO ₃ ²⁻ + H ⁺ = Hfo_wCO ₃ ⁻ + H ₂ O	12.36
Hfo_wOH + CO ₃ ²⁻ + 2H ⁺ = Hfo_wHCO ₃ + H ₂ O	20.412
<i>Carbonate sorption on hematite</i>	
Hfo_wOH + CO ₃ ²⁻ + H ⁺ = Hfo_wCO ₃ ⁻ + H ₂ O	10.92
Hfo_wOH + CO ₃ ²⁻ + 2H ⁺ = Hfo_wHCO ₃ + H ₂ O	22.94

277

278



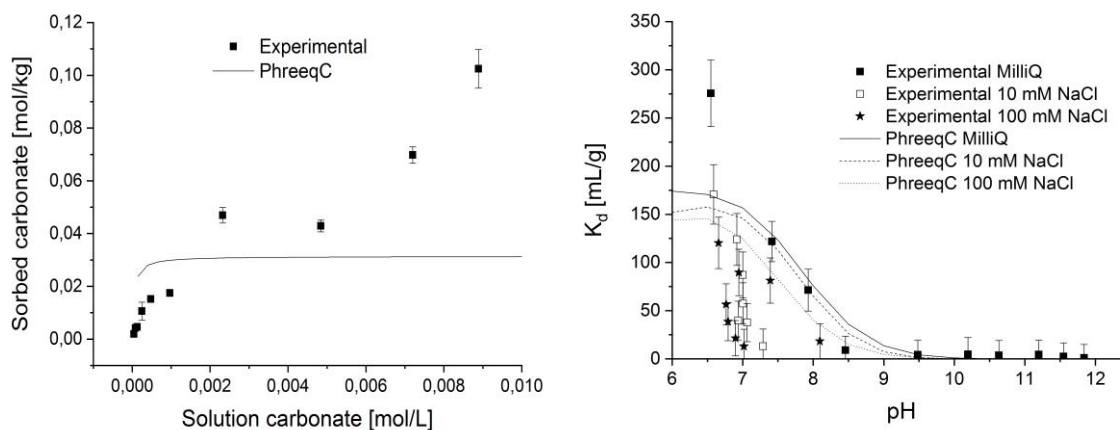
279

280

Fig. 5 The modelled sorption isotherms of carbonate on goethite.

281

282 The generalized double-layer surface complexation model reproduced the sorption results
 283 of carbonate on hematite rather adequately (Fig 6). The surface complexation constants
 284 obtained from the fitting (10.92 and 22.94) were the same as the values (10.92 and 21.94)
 285 obtained by Brechbühl et al. [14] in a similar study while the sorption site density used in
 286 this study 0.30 sites/nm^2 was considerably smaller than 12 sites/nm^2 used by Brechbühl et
 287 al. [14].



288

289

Fig. 6 The modelled sorption isotherms of carbonate on hematite.

290

291 **Conclusions**

292 Carbonate was found to be considerably sorbed on goethite and hematite, but the sorption
293 on magnetite was negligible in all studied conditions. Sorption on goethite and hematite
294 was largest in the neutral pH-range and it decreased with increasing pH. This is caused by
295 the decreasing positive charge of the mineral surface as the pH increases. As pH
296 decreases the speciation of carbon changes from carbonate to bicarbonate and finally to
297 carbon dioxide decreasing the sorption, as the bicarbonate is less preferred compared to
298 carbonate. Carbonate sorption was also observed to slightly decrease with increasing
299 ionic strength, which can be due to the saturation of sorption sites caused by the
300 interactions of chloride ions on the plane typically occupied by electrolyte outer-sphere
301 complexes. The batch sorption results were modelled with the generalized double-layer
302 surface complexation model and the model was able to reproduce rather well the
303 experimental sorption results.

304 Considering the long-term consequences of the final disposal of spent nuclear fuel, we
305 may conclude that radiocarbon is not completely non-sorbing as presently is assumed in
306 conservative safety analyses. In addition to isotopic exchange reaction of carbonate with
307 calcite the sorption on iron oxides is a retarding process preventing rapid migration of
308 radiocarbon into the biosphere.

309 **Acknowledgements**

310 The research leading to these results received funding from the Finnish Research
311 Program on Nuclear Waste Management KYT2018.

312 **References**

- 313 1. Hjerpe T, Ikonen ATK, Broed R (2009) Biosphere assessment report 2009, Posiva
314 Oy, Posiva Report 2010-03.

- 315 2. Posiva. (2013) Safety Case for the Disposal of Spent Nuclear Fuel at Olkiluoto -
316 Models and Data for the Repository System 2012. Posiva Oy, Posiva Report
317 2013-01.
- 318 3. Johnson L, Poinssot C, Ferry C, Lovera P (2004) Estimates of the Instant Release
319 Fraction for UO₂ and MOX fuel at t=0. NAGRA Technical Report 04-08.
- 320 4. Limer LMC, Smith K, Albrecht A, Marang L, Norris S, Smith GM, Thorne MC
321 and Xu S (2012) C-14 Long-Term Dose Assessment: Data Review, Scenario
322 Development, and Model Comparison. Strålsäkerhetsmyndigheten, 2012:47.
- 323 5. Deng B, Campbell TJ, Burris TR. (1997) Hydrocarbon Formation in Metallic
324 Iron/water Systems. *Environ Sci Technol* 31: 1185-1190.
- 325 6. Kaneko S, Tanabe H, Sasoh M, Takahashi R, Shibano T, Tateyama S (2003) A
326 Study on the Chemical Forms and Migration Behavior of Carbon-14 Leached
327 from the Simulated Hull Waste in the Underground Condition. *Mat Res Soc*
328 *Symp Proc*, Vol. 757: 621-626.
- 329 7. Pitkänen P, Partamies S (2007), Origin and Implications of Dissolved Gases in
330 Groundwater at Olkiluoto, Posiva Oy, Posiva Report 2007-04.
- 331 8. Aaltonen I, Engström J, Front K, Gehör S, Kosunen P, Kärki A, Mattila J,
332 Paananen M, Paulamäki S. (2016) Geology of Olkiluoto. Posiva Oy, Posiva
333 Report 2016-16.
- 334 9. Gonfiantini R, Zuppi GM (2003) Carbon Isotope Exchange Rate of DIC in Karst
335 Groundwater. *Chem Geology* 197: 319-336.
- 336 10. Lempinen J, Lehto J (2016) Rate of Radiocarbon Retention onto Calcite by
337 Isotope Exchange. *Radiochim Acta* 104(9): 663-671.
- 338 11. Van Geen A, Robertson AP, Leckie JO (1994) Complexation of Carbonate
339 Species at the Goethite Surface: Implications for Adsorption of Metal Ions in
340 Natural Waters. *Geochim Cosmochim Acta* 58: 2073-2086.
- 341 12. Wijnja H, Schulthess CP (2001) Carbonate Adsorption Mechanism on Goethite
342 Studied with ATR-FTIR, DRIFT, and Proton Coadsorption Measurements. *Soil*
343 *Sci Soc Am J* 65: 324-330.
- 344 13. Villalobos M, Leckie JO (2001) Surface Complexation Modeling and FTIR Study
345 of Carbonate Adsorption to goethite. *J Colloid Int Sci* 235: 15-32.

- 346 14. Brechbühl Y, Christl I, Elzinga EJ, Kretzschmar R (2012) Competitive Sorption
347 of Carbonate and Arsenic to Hematite: Combined ATR-FTIR and Batch
348 Experiments, *J Colloid Int Sci* 377: 313-321.
- 349 15. Cornell, R.M., Schwertmann, U.(2003), *The Iron Oxides*, Wiley-VCH.
- 350 16. Appelo CAJ, Van Der Weiden MJJ, Tournassat C, Charlet L (2002) Surface
351 Complexation of Ferrous Iron and Carbonate on Ferrihydrite and the Mobilization
352 of Arsenic. *Environ Sci Technol* 36: 3096-3103.
- 353 17. Dzombak D.A and Morel F.M.M. (1990) *Surface Complexation Modelling:*
354 *Hydrous Ferric Oxide*. John Wiley & Sons, Inc.